Geomechanics and Engineering, *Vol. 11, No. 2 (2016) 197-209*
DOI: http://dx.doi.org/10.12989/gae.2016.11.2.197

Study of physical simulation of electrochemical modification of clayey rock

Zhaoyun Chai [*1,2], Yatiao Zhang [1] and Alexander Scheuermann [2]

[1] *Mining Technology Institute, Taiyuan University of Technology, Taiyuan, Shanxi 030024, China*
[2] *School of Civil Engineering, the University of Queensland, Brisbane, 4067, Australia*

(*Received January 28, 2015, Revised February 01, 2016, Accepted April 22, 2016*)

Abstract. Clayey rock has large clay mineral content. When in contact with water, this expands considerably and may present a significant hazard to the stability of the rock in geotechnical engineering applications. This is particularly important in the present work, which focused on mitigating some unwelcomed properties of clayey rock. Changes in its physical properties were simulated by subjecting the rock to a low voltage direct current (DC) using copper, steel and aluminum electrodes. The modified mechanism of the coupled electrical and chemical fields acting on the clayey rock was analyzed. It was concluded that the essence of clayey rock electrochemical modification is the electrokinetic effect of the DC field, together with the coupled hydraulic and electrical potential gradients in fine-grained clayey rock, including ion migration, electrophoresis and electro-osmosis. The aluminum cathodes were corroded and generated gibbsite at the anode; the steel and copper cathodes showed no obvious change. The electrical resistivity and uniaxial compressive strength (UCS) of the modified specimens from the anode, intermediate and cathode zones tended to decrease. Samples taken from these zones showed a positive correlation between electric resistivity and UCS.

Keywords: clayey rock; modified mechanism; electrokinetic effect; physical simulation; long-term stability

1. Introduction

Clayey rock is a very commonly occurring rock that may exhibit considerable volume change and breakdown upon contact with water. This behavior is frequently encountered in geotechnical engineering situations and has a considerable influence on the long-term stability of underground excavations (Jeng *et al*. 2002, Alejano *et al*. 2009, Corkum and Martin 2007, Shao *et al*. 2005, Erguler and Ulusay 2009, Pham *et al*. 2007, Hideo 2004). Most existing theories and methods of controlling the stability of weak rock during engineering projects have focused on passive support and anchorage, which involve changing the external properties presented by the rock; however, such strategies have considerable limitations and timeliness. Current research, presently in the experimental investigation phase, has addressed the long-term stability of weak rock in an engineering project context by improving the physical and mechanical properties of the rock.

Relevant areas of study have shown that the modification of rock by electrochemical methods is an effective management strategy (Mikhajlovich 2001, 2006). Pinzari (1962) modified the

*Corresponding author, Ph.D., E-mail: chaizhaoyun_2002@163.com

 ISSN: 2005-307X (Print), 2092-6219 (Online)

mudstone core in coal measure rocks using an electrochemical method, improving the tensile strength of the modified core by a factor of 3.3. Chilingar (1970) and Aggour *et al*. (1992, 1994) studied the effects of a direct electrical current on the permeability of sandstone and oil shale cores. Their results indicated that the permeability of both rock types increased with increasing electrical potential gradient, found to be related to the types and content of clay minerals, with smectite having the greatest effect, followed by illite, then kaolinite. Further studies have conclusively shown that changes occur in the crystal structures, and that the interlamellar spacing of the rock minerals decreases, when a current travels through core specimens. Bernabeu *et al*. (2001) studied the porous system of Bateig stone, and showed that electrochemical treatment consolidated porous rocks, prevented decay and improved its resistance to water and weathering.

The literature on the subject (e.g., Wang *et al*. 2009) contains studies of the subsidence and expandability of clayey rock particles subjected to electrochemical treatment. Results indicate that treatment by direct current alters the subsidence rate of clayey rock particles in distilled water, but its volume expansion is not affected when the subsidence is in a stable state. Also, an electric gradient of 0.5 V/cm provides sufficient electromotive force for the subsidence and the expandability of clayey rock particles. Studies of the pore structure and tensile strength of clayey rock (Wang *et al*. 2009, 2011) have shown that, after electrochemical treatment, the mean tensile strength increased by 16.79%-116.03%, the total pore volume decreased from 33.169 mm^3/g to 9.738-20.215 mm^3/g at the same time as the average pore diameter increased from 6.061 nm to 10.158-21.275 nm, and that the porosity of the modified specimen decreased in the anodic zone and increased in the cathodic zone. However, the previous laboratory test result (Arya and Ian 2013) showed that an increase pore volume with increasing mean particle size. This difference occurred because the amounts of pore decreased considerly after electrochemical treatment. These studies provide references for others to understand the changes of physical properties of clayey rock that result from electrochemical treatment, and to further relate this to engineering applications.

The present study included investigation of the erosion of three electrode metals and differences in current, resistivity and uniaxial compressive strength (UCS) from physical simulation tests. The electrochemical modification mechanism was also analyzed.

2. Model design and implementation

2.1 Experimental apparatus

The experimental apparatus comprised a chamber for the specimen, an electrode, a direct current (DC) power supply, an ammeter, and wire (Fig. 1). The chamber itself consisted of a clear organic glass (acrylic) box of 12 mm wall thickness and 600 mm × 400 mm × 250 mm internal dimensions. A detachable base board had 20 × 10 mm pre-drilled holes for the metal electrodes in each test; the holes simultaneously allowed for water to seep out of tank. To enhance its strength, the box was transversely stiffened by plates glued to each of its four sides. The electrodes were rods of copper (2.25 mm dia.), steel (8 mm dia.) and aluminum (8 mm dia.). The DC power supply provided a voltage output ranging from 0 to 110 V and a maximum current of 3 A. The wire is an ASTVR $\Phi 35\times 1$ mm^2 silk-covered wire.

2.2 Model materials and proportions

The prototype specimen of a lacustrine facies clastic sedimentary rock from the Cenozoic

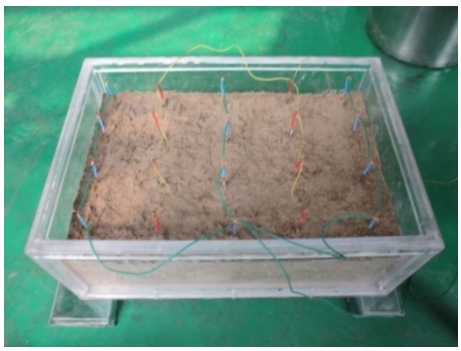

Fig. 1 Wire connection in model (blue = anode; red = cathode)

Palaeogene Lijiaya Formation was taken Wali coal mine, Shangdong Province, China. The specimen showed obvious laminar structure, exchangeable positive ions were K+, Na+, Ca2+ and Mg2+, the capacity was 42.5 meq/100g, the bulk density was 2500kg/m3, and moisture content was 23.54%. The contents of smectite, illite, chlorite, quartz, anorthose, calcite, pyrite and dolomite in the sample was 20%, 10%, 10%, 40%, 10%, 5%, 3% and 2% respectively (Chai *et al*. 2014a, b). The major consideration is the similarity of mineralogical composition between model materials and prototype when model materials were selected, combined with measured results of free swelling tests on prototype samples (Chai *et al*. 2014a), and make a final determination of the major components of the model material were sand, bentonite and gypsum in the proportions 7:1.5:1 by weight.

2.3 Experimental method

Three models were tested, each with electrodes of copper, steel or aluminum. The electrodes were positioned with similar electrodes 100 mm apart, and different electrodes 125 mm apart. The distance from the electrodes to the inner wall of the chamber was 50 mm. The simulation materials were laid in the box in ten horizontal layers 15 mm thick. After each layer was placed, a steel plate 20 mm thick with a handle welded to it and with 10 mm diameter holes corresponding to the electrode positions, was placed on the layer. To ensure uniform compaction of the model material around the electrodes, a 5 kg drop-hammer was then dropped onto the handle of the plate using a fixed number of hits from a fixed height, then removed steel plate laid next layer.

Once this work was complete, the wires were connected as shown in Fig. 1, and 6.3 V DC was applied at an electrical potential gradient of 0.5 V/cm. Plastic wrap was then placed on the surface of the model materials to minimize the effects of evaporation on the model material.

3. Experimental results and analysis

3.1 Experimental observations

The observed effects around the anode and cathode are shown in Fig. 2. The copper anodes produced a roughly cylindrical zone of bronze-green material (Fig. 2(a)). Around the cathode, a few white flocculent crystals were generated on the surface, but no change was observed in the vertical section, as shown in Fig. 2(b).

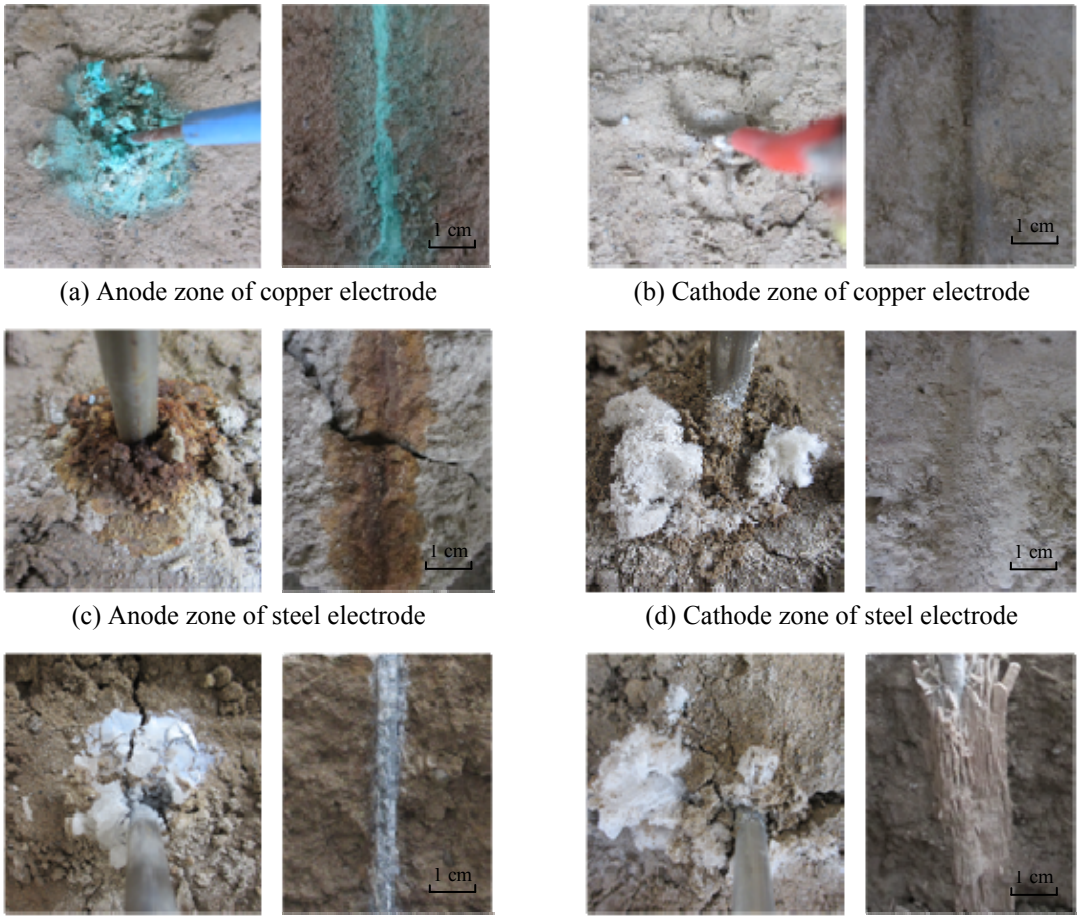

(a) Anode zone of copper electrode (b) Cathode zone of copper electrode

(c) Anode zone of steel electrode (d) Cathode zone of steel electrode

(e) Anode zone of aluminum electrode (f) Cathode zone of aluminum electrode

Fig. 2 Observed results of physical model experiments

The effect at the steel anode was similar to that at the copper anode, except for the rusty red color as shown in Figs. 2(c)-(d).

At the aluminum anode a few white, glassy crystals were generated that had risen to the surface through cracks around it, and white crystals were found in vertical section, but the amount was far less than it was the case for either the copper or steel anodes (Fig. 2(e)). A few white flocculent crystals had risen to the surface through cracks around the cathode, and in the vertical section a regular radial zone of gray-striped new mineral was found around the cathode (Fig. 2(f)).

3.2 New minerals

The effect of applying a DC to the models is to electrolyze water molecules, with oxidation in the anodic zone producing oxygen, and reduction in the cathodic zone producing hydrogen. The reaction equations (Acar and Alshawabkeh 1993) are

$$\text{Anodic zone:} \qquad 2H_2O - 4e^- \rightarrow O_2 \uparrow + 4H + \tag{1}$$

$$\text{Cathodic zone:} \qquad 2H_2O + 2e^- \rightarrow H_2 \uparrow + 2OH^- \tag{2}$$

Electrolysis therefore alters the pH in the model materials such that the acid materials migrate towards the cathode, and the base materials migrate towards the anode. The acid front moves faster than the base front due to the higher mobility of H^+ than OH^-, as a result, the acid front dominates the chemistry across the model materials except for some small parts close to the cathode (Nasim *et al*. 2012). A large pH gradient is created in the neutralized region of H^+ and OH^-, with the materials dewatering and consolidating. The reaction equation is

$$H^+ + OH^- \rightarrow H_2O \tag{3}$$

At the same time, a metal oxidation reaction occurs at the anode under acid conditions

$$M - ne^- \rightarrow M^{n+} \tag{4}$$

The metal electrodes are corroded and new minerals are generated, as shown in Fig. 3. X-ray diffraction (XRD) analysis was performed on model materials specimen to assess sample mineralogy (see Fig. 4). The XRD results are given in Table 1.

At the surface of the cathodic zones, silicon oxide and aluminum oxide combination reacted with the molecule forming white, flocculent allophone. A small amount of $Cu(OH)_2$ was created at the surface of the copper cathode in basic conditions, which further decomposed to black CuO and adhered to the surface of the electrode, as seen in Fig. 3(a). The steel cathode did not undergo basic change, as shown in Fig. 3(b). For the aluminum electrodes, a large, regular, radially distributed zone of gray striped gibbsite was produced around the anode, as shown in Fig. 3(c).

Corrosion of the copper and steel electrodes is clearly seen to have occurred mainly at the anodes, with a greater amount of corrosion of the copper than the steel; however, for aluminum, both electrodes were corroded to some extent, although the cathode showed far more corrosion than the anode. Considering both economic and engineering applicability, steel was selected as the

Table 1 New mineral in cathodic and anodic zone

Electrode	Electrode material		
	Copper	Steel	aluminum
Anode	basic cupric carbonate, $Cu(OH)_2$, CuO	Fe_2O_3, Fe_3O_4	Gismondine, kyanite
Cathode	$Cu(OH)_2$, CuO, allophane*	Allophane*	Gibbsite, allophane

(a) Copper (b) Steel (c) Aluminum

Fig. 3 Observed corrosion of electrodes

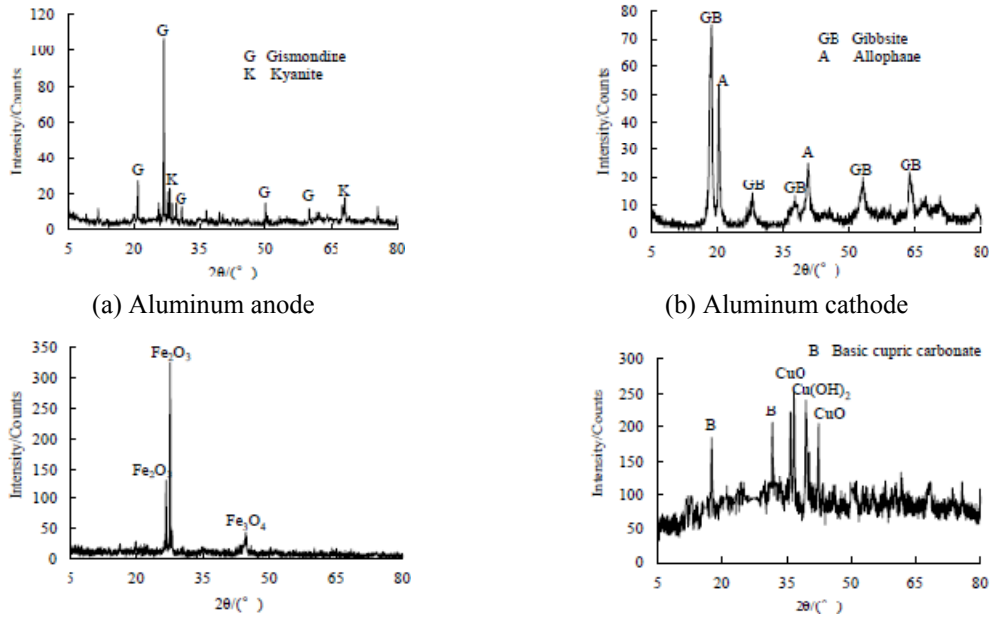

(a) Aluminum anode (b) Aluminum cathode

(c) Steel anode (d) Copper athode

Fig. 4 The X-ray diffraction pattern of new mineral in cathodic and anodic zone

electrode material for applying electrochemical modification for long-term stability control of clayey rock. This is consistent with the fact that steel is used for bolts and cables in rock engineering.

3.3 Change of electrical current

The relationship between electrical current and treatment time for the three electrode materials is shown in Fig. 5. The initial currents applied to the copper, steel and aluminum electrodes were 0.22 A, 0.21 A and 0.19 A, respectively. Initially the current vs. treatment time curves decreased abruptly for all three electrode materials. This trend is caused by temperature rose at the anode, and the model materials in contact with anodes started to desiccate, becoming less and less conductive and resulting in a deterioration of the electrical contact between the anodes and the model materials. Soft clay electro-osmotic consolidation studies by Burnotte *et al*. (2004) have produced similar results. For the copper electrodes, the current decreased abruptly after remained at approximately 0.16 A for nearly 80 h before again dropping. The gradient decreased until a stable value of 0.03 A was reached, a decrease of 86.4%. For the steel electrodes, the current remained at approximately 0.11 A for nearly 40 h before again falling, then the gradient decreased to a stable value 0.07 A, a decrease of 66.7%. For the aluminum electrodes, however, the current did not display an intermediate steady state, but rather the gradient immediately began to decrease to a stable value of 0.03 A, a decrease of 84.2%.

3.4 Electric resistivity

Following the above experiment, prismatic test specimens measuring approximately 50 mm × 50 mm × 100 mm were cut from the tested material in the anodic, intermediate and cathodic zones

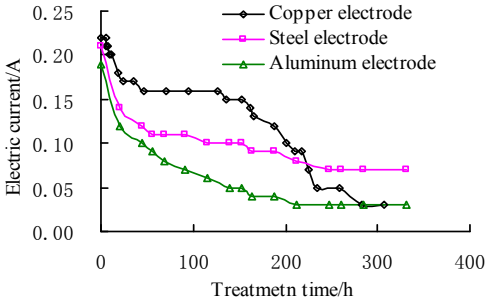

Fig. 5 Electrical current vs. treatment time for the three electrode materials

of the models. The surface of the specimens was then polished and covered with a thin layer of graphite to increase conductivity, and copper electrodes were clamped in position to ensure close contact. A TH2828A digital alternating current (AC) bridge (Huizhou, China) was selected to measure electric resistivity at a test voltage of 5 mV. Then, the mechanical compressive strength was determined using a JL-WAW 60 PC-controlled electro-hydraulic servo universal testing machine (Jilin Test Technology, Changchun, China), which had a maximum load capacity of 6.0×10^4 kg and minimum displacement rate 1.0×10^{-3} mm/s. The servo control system allowed the loading rate to be varied.

Fig. 6 shows the measured curves of electrical resistivity for the three electrode materials. The following can be seen. (1) The electrical resistivity decreased as the test frequency increased, in accordance with a negative algorithmic law. The fitted equation is written as

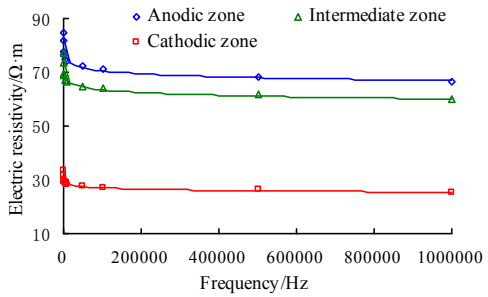

(a) Copper electrode

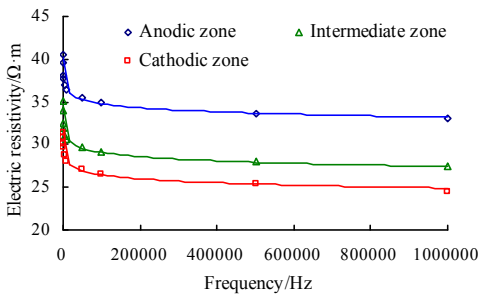

(b) Steel electrode

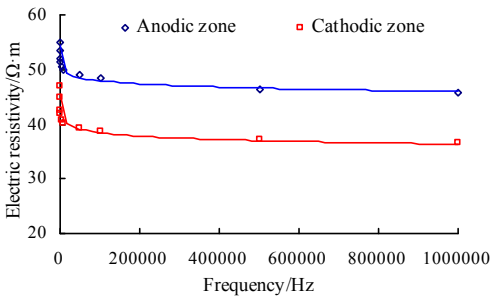

(c) Aluminum electrode

Fig. 6 The electrical resistivity for different electrode materials

Table 2 Fitted parameters and correlation coefficients

Electrode material	Sampling area	A	B	Correlation coefficients R^2
Copper	Anode	0.6994	42.861	0.9901
	Intermediate	0.7157	37.318	0.9842
	Cathode	0.6711	34.189	0.9918
Steel	Anode	1.5947	88.890	0.9728
	Intermediate	1.4590	80.239	0.9524
	Cathode	0.6937	34.991	0.9540
Aluminum	Anode	0.8385	57.599	0.9856
	Cathode	0.9201	49.058	0.9605

$$\rho_s = -A\ln(f_e) + B \tag{5}$$

Where, ρ_s is the electrical resistivity; f_e is the test frequency; and A, B are fitted parameters. The values of A and B and correlation coefficients for all specimens are listed in Table 2.

(2) The trend of the electrical resistivity of the specimens from the different zones is anode > intermediate > cathode. These differences are the result of the electrochemically altered porosity of the specimens. When a DC is applied to specimens, it stimulates the migration of electricity, pore fluid, ions and fine particles across the specimens towards the oppositely charged electrode, thus creating combined effects of a chemical, hydraulic and electrical (CHE) gradients. The migration of the pore fluid from anode to cathode through the capillary influence of an electric field, and caused anodic zone consolidation after loss of water. The motion of negatively charged particles (usually micelles or colloids) relative to a fluid under an electric gradient, agglomerate and coarsen on anodic zone, tending to fill the pores and reducing the porosity, thus increasing both the compactness and the electrical resistivity of the specimen. While the gradual movement of the positively ions or charged electrical species under an electric gradient, increases the degree of electro-osmosis and electrolytic process, further caused the porosity of cathodic zone increased. This has been confirmed by the previous laboratory test results (Wang *et al*. 2009, 2011).

Lo *et al*. (1991) reported that, if the electrode is reversed after a certain period of treatment time, the strength of the specimen can be increased more and the improvement can be extended from the anode to the cathode, further cancel out the inhomogeneity drawbacks. However, Ou *et al*. (2009) laboratory and field tests results showed that polarity reversal is not for electroosmotic chemical treatment.

3.5 UCS

The stress-strain curves and results of the UCS tests on the specimens from different zones of the model after electrochemical modification are shown in Fig. 7 and Table 3, respectively. The trend of the UCS was anode > intermediate > cathode for all the electrode materials, as below. For the copper electrodes, the average UCS of specimens from the anodic zone was 1.501 MPa, i.e., 2.0 times the value in the intermediate zone and 3.2 times the value in the cathodic zone. For the steel electrodes, the average UCS of specimens from the anodic zone was 0.846 MPa, i.e., 1.3 times the value in the intermediate zone and 2.5 times the value in the cathodic zone. For the aluminum electrodes, the average UCS of specimens from anodic zone was 0.688 MPa, i.e., 1.9 time the value in the cathodic zone.

Table 3 UCS test results

Electrode material	Sampling area	UCS/MPa			
		No. 1	No. 2	No. 3	Average
Copper	Anode	1.677*	1.325	-	1.501
	Intermediate	0.989*	0.869	0.384	0.747
	Cathode	0.612*	0.373	0.421	0.468
Steel	Anode	0.737	0.955*	-	0.846
	Intermediate	0.720*	0.553	-	0.637
	Cathode	0.431*	0.243	-	0.337
Aluminum	Anode	0.985	0.546*	0.854	0.795
	Cathode	0.534	0.426*	0.295	0.418

* UCS determined following electrical resistivity test

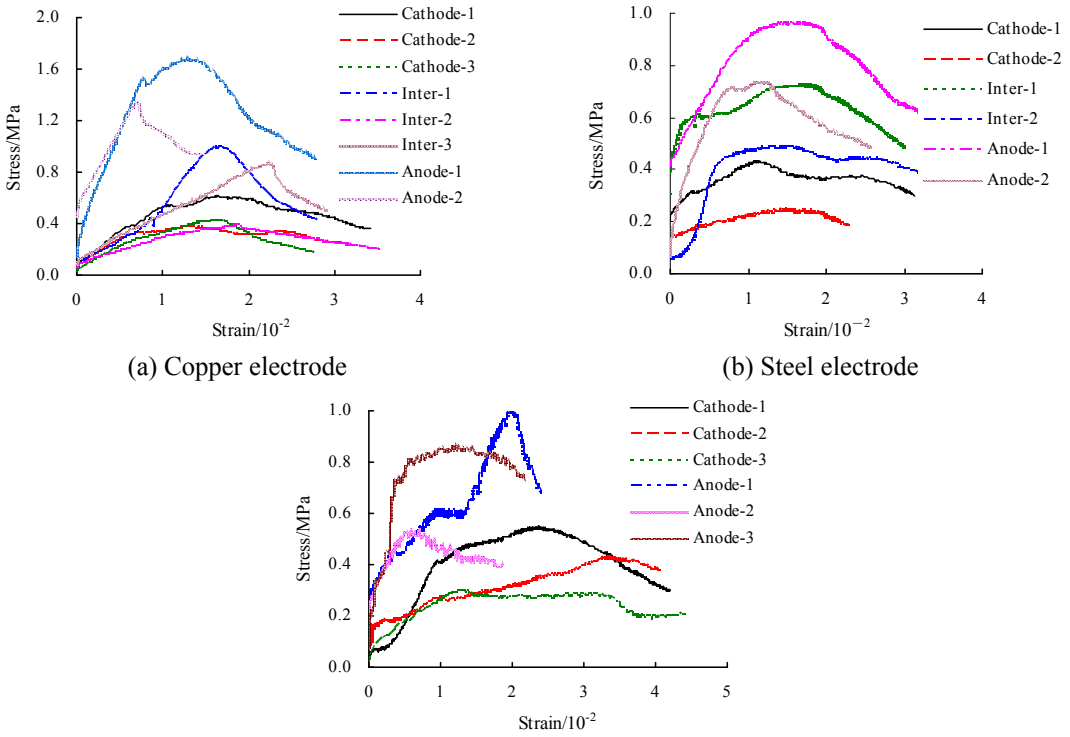

(a) Copper electrode

(b) Steel electrode

(c) Aluminum electrode

Fig. 7 The stress-strain curves of specimens from different model materials

Some actions contributing to these results include (i) electrolysis causes obvious changes to the mineralogical composition of the clay and silicate minerals; (ii) anaphoresis and electro-osmosis causes marked changes in the pore structure by forcing the positively charged polar water molecules to migrate to the cathode, which in turn reduces the hydrated layer and the hydrophilicity; and (iii) dehydration and consolidation of the anodic zone increase the intermole-

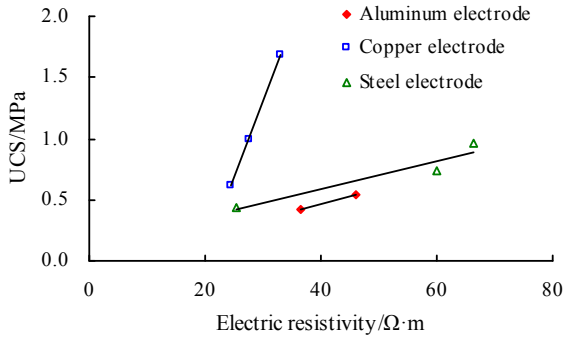

Fig. 8 Relationship between UCS and electrical resistivity for the three types of electrode

cular and hydrogen bond forces, thus enhancing the cohesive and interconnective forces at the same time as they improve the cementation properties of the clay mineral particles.

4. Correlation between electrical resistivity and UCS

The relationship between the electrical resistivity and the UCS of specimens for the three electrode materials are shown in Fig. 8. The following can be seen.

(1) Overall, the relationship between UCS and electrical resistivity is difficult to quantify by a particular functional relationship since the test date may play a role as well.
(2) For the copper and steel electrodes, the UCS of the specimen monotonically increased as electrical resistivity increased. A similar result was reported by Dong *et al*. (2014) in studies of the relationship between the strength and electrical resistivity of cemented soil. This indicates that strength change may be determined from change in electric resistivity for the same categories of material.

5. Analysis of electrochemical modification mechanism

The essence of clayey rock electrochemical modification is the electrokinetic effect of a DC electrical field on the clayey rock, combined with the coupling effect between the hydraulic and electrical potential gradients in fine-grained rock (Acar and Alshawabkeh 1993). These effects occur due to the presence of a diffuse double layer around the fine clay particles (Mitchell 1993), and involve the movement of electrically charged particles and fluids. The electrokinetic effect in clayey rock mainly includes electro-osmosis, electrophoresis and electromigration (or ion migration) as illustrated in Fig. 9. When an electrical current is applied via electrodes implanted in clayey rock, pore water electrolysis reactions dominate the chemistry around the electrodes, resulting in oxidation at the anode and generating an acidic front. Similarly, reduction at the cathode produces a base front. This generates an electric potential gradient and acid-base gradient between the electrodes, causing electrokinetic effects. The positively charged polar water molecules inside the anodic zone migrate to the cathode and are neutralized during the migration process. Thus the moisture content of the specimen is reduced by dehydration.

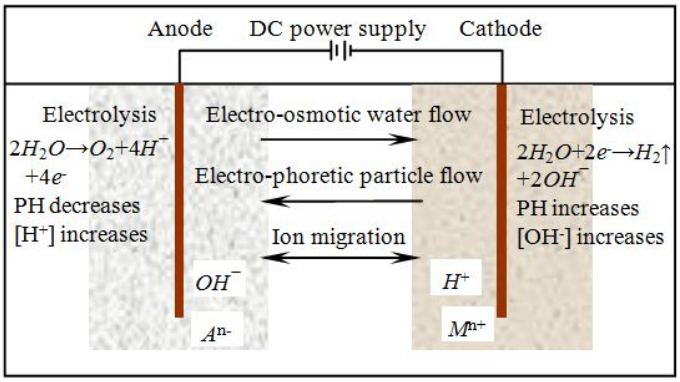

Fig. 9 Electrokinetic effects in clayey rock

At the same time, suspended micelles or colloidal particles within the fluid medium also migrate to the anode, agglomerating and coarsening and filling the pores thus the porosity of the specimen decreases. At the same time, ion migration occurs within the fluid phase of the charged particle matrix, so that positively charged particles such as H^+ and M^{n+} move towards the cathodic zone, and negatively charged particles such as OH^- and A^{n-} migrate towards the anodic zone. These react to form new minerals, further enhancing the strength of the clayey rock.

6. Conclusions

(1) After a DC was applied to the clayey rock, the metal electrodes were oxidized and new minerals were generated at the anodes. Aluminum electrodes were corroded and gibbsite were generated. Steel and copper electrodes showed no obvious change at the cathode.
(2) When the DC was initially applied, the current vs. treatment time curves for all three electrode materials abruptly decreased. The gradient decreased until a stable value was reached.
(3) The trend of electrical resistivity and UCS of the modified specimens from all electrode zones was found to be anode > intermediate > cathode. A positive correlation was found between electric resistivity and UCS for each electrode material.
(4) The essence of clayey rock electrochemical modification is the electrokinetic effect of the DC field, together with the coupled hydraulic and electrical potential gradients in fine-grained clayey rock. These effects include ion migration, electrophoresis and electro-osmosis.

Acknowledgments

This work was supported by the National Natural Science Foundation of China, grant no. 51004075 and 50974093, by Shanxi Province Science Foundation for Youths, grant no. 2011021024-2, and by Shanxi Province Excellence Youths Academic Leader Supported Program, grant no. 2012.

References

Acar, Y.B. and Alshawabkeh, A.K. (1993), "Principles of electrokinetic remediation", *Environ. Sci. Technol.*, **37**(13), 2638-2647.

Aggour, M.A. and Muhammadain, A.M. (1992), "Investigation of water-flooding under the effect of electrical potential gradient", *J. Petrol. Sci. Eng.*, **7**(3/4), 319-327.

Aggour, M.A., Tchelepi, H.A. and Yousef, H.Y. (1994), "Effect of electroosmosis on relative permeability of sandstones", *J. Petrol. Sci. Eng.*, **11**(2), 91-102.

Alejano, L.R., Rodriguez-Dono, A., Alonso, E. and Fdez-Manin, G. (2009), "Ground reaction curves for tunnels excavated in different quality rock masses showing several types of post-failure behaviour", *Tunn. Undergr. Space Technol.*, **24**(6), 689-705.

Arya, A.L. and Ian, J. (2013), "Collapsibility in calcareous clayey loess: A factor of stresss-hydraulic history", *Int. J. GEOMATE*, **5**(1), 620-627.

Bernabeu, A., Expósito, E., Montiel, V., Ordóñez, S. and Aldaz, A. (2001), "A new electrochemical method for consolidation of porous rocks", *Electrochem. Commun.*, **3**(3), 122-127.

Burnotte, F., Lefebvre, G. and Grondin, G. (2004), "A case record of electroosmotic consolidation of soft clay with improved soil-electrode contact", *Can. Geotech. J.*, **41**(6), 1038-1053.

Chai, Z.Y., Kang, T.H. and Feng, G.R. (2014a), "Effect of aqueous solution chemistry on the swelling of clayey rock", *Appl. Clay Sci.*, **48**(93/94), 12-15.

Chai, Z.Y., Kang, T.H. and Chen, W.Y. (2014b), "Effects of organic silicone additive material on physical and mechanical properties of mudstone", *Geomech. Eng., Int. J.*, **6**(2), 139-151.

Chilingar, G. (1970), "Effect of direct electrical current on permeability of sandstone cores", *J. Pet. Technol.*, **22**(7), 8-17.

Corkum, A.G. and Martin, C.D. (2007), "The mechanical behaviour of weak mudstone (Opalinus Clay) at low stresses", *Int. J. Rock Mech. Min. Sci.*, **44**(2), 196-209.

Dong, X., Su, N., Huang, X. and Bai, X. (2014) "Effect of sewage on electrical resistivity and strength of cemented soil", *Rock Soil Mech.*, **35**(7), 1855-1862.

Erguler, Z.A. and Ulusay, R. (2009), "Water-induced variations in mechanical properties of clay-bearing rocks", *Int. J. Rock Mech. Min. Sci.*, **46**(2), 355-370.

Hideo, K. (2004), "Simplified evaluation for swelling characteristics of Bentonites", *Eng. Geol.*, **71**(3/4), 265-279.

Jeng, F.S., Wang, M.C., Huang, T.H. and Liu, M.L. (2002), "Deformational characteristics of weak sandstone and impact to tunnel deformation", *Tunn. Undergr. Space Technol.*, **17**(3), 263-274.

Lo, K.Y., Inculet, I.I. and Ho, K.S. (1991), "Electroosmotic strengthening of soft sensitive clays", *Can. Geotech. J.* **28**(1),62-73.

Mikhajlovich, P.S. (2001), "Process of electrochemical strengthening of rock", Russia Patent; No. 2299294.

Mikhajlovich, P.S. (2006), "Method for electrochemical rock consolidation", Russia Patent; No. 2175040.

Mitchell, J.K. (1993), *Fundamentals of Soil Bahaviour*, (2nd Ed.), John Wiley & Sons Inc., New York, NY, USA.

Nasim, M., Erwin, O. and Gary, C. (2012), "A review of electrokinetic treatment technique for improving the engineering characteristics of low permeable problematic soils", *Int. J. GEOMATE*, **2**(2), 266-272.

Ou, C., Chien, S. and Chang, H. (2009), "soil improvement using electroosmosis with the injection of chemical soluteions: Field fests", *Can. Geotech. J.*, **46**(6), 727-733.

Pham, Q.T., Vales, F., Malinsky, L., Minh, D.N. and Gharbi, H. (2007), "Effects of desaturation resaturation on mudstone", *Phys. Chem. Earth, Parts A/B/C*, **32**(8-14), 646-655.

Pinzari, U. (1962), "Indagine sul trattamento elettrosmotico di un materiale argilloso", *Geotecnica*, **9**(3), 101-114.

Shao, J.F., Ata, N. and Ozanam, O. (2005), "Study of desaturation and resaturation in brittle rock with anisotropic damage", *Eng. Geol.*, **81**(3), 341-352.

Wang, D., Kang, T., Chai, Z., Han, W. and Liu, Z. (2009), "Experimental studies of subsidence and expandability of montmorillonitic soft rock particles under electrochemical treatment", *Chin. J. Rock.*

Mech. *Eng*., **28**(9), 1876-1883.
Wang, D., Kang, T.H., Han, W.M., Liu, Z.P. and Chai, Z.Y. (2010), "Electrochemical modification of the porosity and zeta potential of montmorillonitic soft rock", *Geomech*. *Eng*., *Int*. *J*., **2**(3), 191-202
Wang, D., Kang, T.H., Han, W.M. and Liu, Z.P. (2011), "Electrochemical modification of tensile strength and pore structure in mudstone", *Int*. *J*. *Rock Mech*. *Min*. *Sci*., **48**(4), 687-692.

CC